Traveling-wave free-electron laser

Eli Jerby
Faculty of Engineering, Tel Aviv University, Ramat Aviv, Israel, 69978
and Research Laboratory of Electronics, Massachusetts Institute of Technology, Cambridge, Massachusetts 02139
(Received 22 January 1990; revised manuscript received 19 February 1991)

The concept of a traveling-wave free-electron laser (TWFEL) is presented. This hybrid device consists of both a periodic waveguide and a planar wiggler. It combines the interaction mechanisms of both the traveling-wave tube (TWT) and the free-electron laser. This combination produces a synergistic interaction. A linear model of the TWFEL is derived in this paper. It results in a general dispersion equation for the TWFEL interaction. Coupling coefficients are derived for various ratios between the wiggler period λ_W and the periodic waveguide period λ_p. It is shown that when $\lambda_W = \lambda_p$ the parametric interaction is composed of a double FEL interaction, a TWT interaction, and a hybrid interaction. All these are in resonance with three different spatial harmonics. The coupling coefficient for this scheme is a complex sum of the known FEL and TWT terms, and of complex terms for their cross coupling. It is shown that the coupling coefficient of the synergistic TWFEL interaction (and consequently its gain) can be larger than the sum of the two separate interactions. Simpler TWFEL schemes in which $\lambda_W \neq \lambda_p$ (single-harmonic interaction) and $\lambda_W = 2\lambda_p$ (two-harmonic interaction) are presented first as an introduction for the analysis of the $\lambda_W = \lambda_p$ TWFEL interaction. A compact TWFEL based on a miniature wiggler, which functions also as a periodic waveguide, is proposed for operation in the millimeter-wave range with a tenuous low-energy e beam.

I. INTRODUCTION

The traveling-wave free-electron laser (TWFEL) is presented in this paper as a hybrid of the traveling-wave tube (TWT) and the Ubitron-type free-electron laser (FEL). The interaction of the electromagnetic wave and the electron beam in this device is a synergism of the known TWT and the FEL mechanisms.

The traveling-wave tube[1] has been known for the past four decades as an efficient amplifier of microwave frequencies. The amplification mechanism of the TWT is based on the electron-beam bunching by a longitudinal, synchronized force. This traveling force wave is produced by the axial electric field component of the slow electromagnetic wave, given by the first term of the Lorentz equation, $F_z = -eE_z$. The TWT slow wave structure is either a helix or a periodic waveguide. Both can support slow electromagnetic waves with phase velocity close to the propagating velocity of the electron beam. This synchronized velocity maintains the stationary phase of the bunching force along the interaction. The bunched e-beam axial ac current, J_z, is coupled to the axial (em) wave component E_z. This coupling results in a stationary $J_z E_z$ product, and it enables efficient energy transfer from the e beam to the em wave.

The Ubitron[2,3] was developed as a millimeter-wave high-power version of the traveling-wave tube. This device differed from the TWT by its fast-wave interaction. The amplified em wave propagates in a uniform waveguide while the e beam is subjected to an external undulator field. The undulator had been used before to produce spontaneous radiation from fast electron beams.[4] It is constructed as a periodic array of static magnetic poles, and it causes a wiggling motion of the e beam. This motion leads to an axial bunching force due to the second term of the Lorentz force, $\mathbf{F}_z = -e\mathbf{V}_{W\perp} \times H_\perp$, where $\mathbf{V}_{W\perp}$ is the perpendicular velocity component of the wiggling motion and $\mathbf{H}_\perp$ is the transverse magnetic component of the em wave. The consequence of this force is an axial bunching, as in the conventional TWT. The FEL amplification, however, is the result of the coupling between the *transverse* wiggling of the bunched electron beam and the transversely polarized em wave. This coupling results in a stationary $\mathbf{J}_\perp \cdot \mathbf{E}_\perp$ product and, consequently, in energy transfer from the e beam to the em wave.

The free-electron laser was proposed,[5] and approved,[6-8] as a mechanism for emission and amplification of much shorter wavelengths, typically in the ir range and shorter. It uses a relativistic high-energy electron beam injected into a wiggler. Due to the wiggling motion, as in the Ubitron, the relativistic e beam interacts with the optical wave, propagating on the same axis in free space. The condition for a velocity synchronism between the bunching force and the e beam leads in the relativistic limit to the relation $\lambda \cong \lambda_W/\gamma^2$, where λ is the optical wavelength, λ_W is the wiggler periodicity, and γ is the relativistic factor.

The Raman FEL (Refs. 9 and 10) employs an intense, high-current electron beam. Its typical e-beam energy is much lower than that of the FEL in the Compton regime. Consequently, its operating wavelength is longer, and is typically in the microwave or the millimeter-wave regime.

Space-charge effects are dominant in the Raman FEL interaction.

FEL schemes which do not employ a magnetic wiggler are based on *slow-wave* interaction. These are the Čerenkov FEL,[11] the Smith-Purcell FEL,[12,13] and their hybridization, the FEL in a periodic dielectric medium.[14]

A free-electron laser which employs both a wiggler and a slow-wave medium is the gas-loaded FEL.[15] Other proposed hybrid devices consisting of wigglers and periodic structures are the two-beam accelerator,[16] the FEL efficiency enhancement by a slow rf field,[17] the periodic dielectric FEL,[18] and recently, the TWFEL (Ref. 19) and the space-charge coupled FEL.[20]

A unified theory for various *fast-wave* and *slow-wave* FEL interactions[21] shows that a dispersion equation similar to the Pierce cubic equation for TWT's (Ref. 1) is valid also for various FEL schemes. The unified dispersion equation is written in the form[21]

$$s(1+\chi_z) - i\kappa\chi_z = 0, \tag{1}$$

where s is the variation in the em wave wave number due to the interaction, χ_z is the longitudinal susceptibility of the e beam, and κ is the coupling coefficient of the interaction. Expressions for the coupling parameter κ and the FEL gain are given in Refs. 21 and 22 for various types of interaction. A wide definition of the free-electron laser could include the TWT and the Ubitron, as well as the various devices mentioned above, as versions of the FEL.

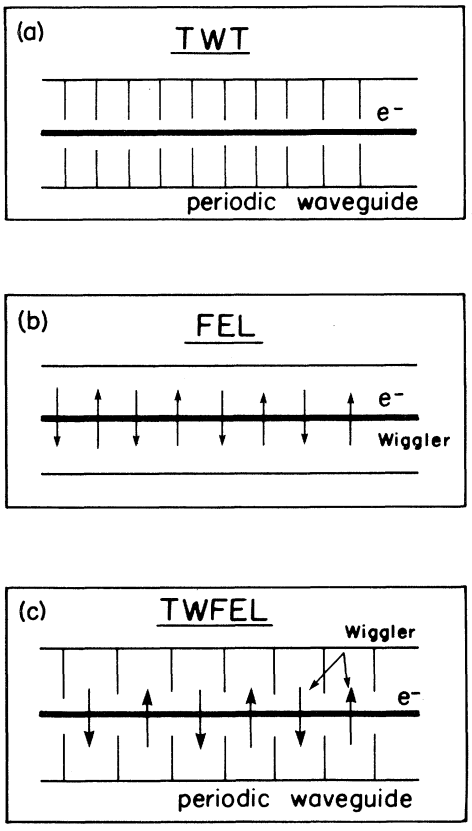

FIG. 1. Figurative schemes of (a) the TWT, (b) the FEL, and (c) the TWFEL.

The traveling-wave free-electron laser[19] is a hybrid of the TWT and the FEL schemes, and it operates as a synergism of both interactions. Figure 1 shows for comparison schemes of a TWT, a FEL, and the TWFEL. The latter consists of both a planar wiggler and a periodic waveguide. The parametric interaction in the hybrid TWFEL device is composed of the two known mechanisms, the TWT and the FEL, in addition to cross-coupled hybrid interactions. In the TWFEL, the Ubitron-FEL interaction is performed by the transverse wave components of the slow harmonics, while the TWT interaction is performed simultaneously by the axial wave component. In the case of $\lambda_W = \lambda_p$, namely, when the wiggler period equals the waveguide period, the combined TWT and FEL bunching force is given symbolically by the threefold Lorentz force expression

$$F_z(\omega,\beta_n)|_{\text{TWFEL}} = -eE_z^{(n)}|_{\text{TWT}} - eV_{Wx}H_y^{(n+1)}|_{\text{FEL1}} - eV_{Wx}H_y^{(n-1)}|_{\text{FEL2}}, \tag{2}$$

where $\beta_n \simeq \omega/V_z$ is the wave number of a spatial harmonic of order n, in synchronism with the TWT interaction, and V_z is the axial velocity of the electron beam. The TWFEL-bunched e beam is driving the em wave by two current components; one is the longitudinal current (which causes a TWT-type excitation) and the other is the transversal current (which causes an FEL-type excitation). Each current component, however, is composed of three terms for the different bunching forces in Eq. (2). Hence the synergistic TWFEL interaction may have a stronger coupling (and consequently a higher gain) than the uncoupled TWT and FEL interactions, because of the possible additional contribution of the cross-coupling interactions. Another advantage of the TWFEL is that it requires a lower e-beam energy than a Ubitron-FEL, because of the interaction with slow waves.

A linear model of the TWFEL is derived in the following sections. As expected, it results in a dispersion equation similar to Eq. (1). The coupling parameter κ is derived for various schemes and is found to be composed of terms related to the known FEL and TWT interactions, in addition to cross-coupling complex terms. Some features of the TWFEL are demonstrated by numerical examples. A TWFEL based on a miniature wiggler is proposed for the millimeter-wave regime. The miniature wiggler in this scheme functions also as the periodic waveguide, hence the condition $\lambda_W = \lambda_p$ can be satisfied in a simple structure.

II. A LINEAR MODEL OF THE TWFEL INTERACTION

The model derived in this section assumes the TWFEL scheme shown in Fig. 2. Two regions are defined in the

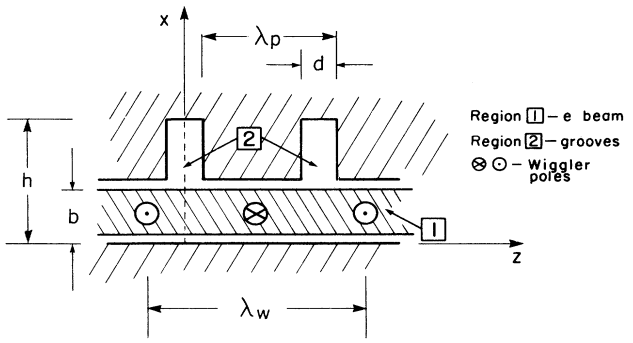

FIG. 2. A scheme of the traveling-wave free-electron laser (TWFEL) model analyzed in this paper.

periodic waveguide. Region 1 is the *channel* $(0 < x < b)$, and region 2 is the groove volume $(b \leq x \leq h)$. A transversely uniform electron beam is propagating in the z direction in the *channel* $(0 < x < b)$, where an ideal planar wiggler field, $\mathbf{B}_w(z) = \hat{\mathbf{y}} B_W \sin(k_W z + \alpha_W)$, is induced. The angle α_W is the relative phase of the wiggler, measured in the center of the first groove, in $z = 0$. It is shown later that α_W has an important role in tuning the TWFEL interaction.

Using a known solution for the fields in the empty periodic waveguide, we perform a perturbation analysis, assuming a slow varying amplitude interaction. This results in a general dispersion equation for the TWFEL interaction, from which we derive the growth rates for various TWFEL schemes.

A. Harmonics in a periodic waveguide

A known solution for the empty periodic waveguide[23] is assumed here as the zeroth-order solution for the fields evolved in the TWFEL periodic waveguide shown in Fig. 2. The TM waves in the *channel* $(0 \leq x \leq b)$ are described (in the absence of the e beam) by a spatial harmonic decomposition. The transverse field components are written as

$$E_{xo} = A_0 \sum_n e_{xn} \phi_{cn}(x) e^{i\beta_n z}, \tag{3a}$$

$$H_{yo} = A_0 \sum_n h_{yn} \phi_{cn}(x) e^{i\beta_n z}, \tag{3b}$$

and the longitudinal electric field component is

$$E_{zo} = A_0 \sum_n e_{zn} \phi_{sn}(x) e^{i\beta_n z}. \tag{3c}$$

The transverse functions $\phi_{cn}(x)$, $\phi_{sn}(x)$ are given by

$$\phi_{cn}(x) = \frac{\cosh(\gamma_n x)}{\cosh(\gamma_n b)}, \tag{3d}$$

$$\phi_{sn}(x) = \frac{\sinh(\gamma_n x)}{\sinh(\gamma_n b)}, \tag{3e}$$

where $\gamma_n = \sqrt{\beta_n^2 - k^2}$ is the harmonic decaying rate in the x dimension. The harmonic wave number is $\beta_n = \beta_0 + n\beta_p$, where $\beta_p = 2\pi/\lambda_p$ is the waveguide periodicity.

Inside the groove $(b \leq x \leq h)$ we assume a standing TEM wave in the x direction, as follows:

$$E_{zo} = A_0 \sin k(h - x), \tag{4a}$$

$$H_{yo} = i\sqrt{\epsilon_0/\mu_0} A \cos k(h - x). \tag{4b}$$

This description is limited to narrow grooves $(b < \lambda)$. Otherwise, a multimode analysis for the periodic waveguide should be included in the model.[24]

The wave continuity between regions 1 and 2 (in $x = b$; $-d/2 \leq z \leq d/2$) leads to a dispersion equation (ω, β_0) from which the wave number β_0 is derived for a given angular frequency ω. It also determines the field coefficient e_{zn} for the various harmonics as follows:

$$e_{zn} = \sin k(h - b) \frac{d}{\lambda_p} \frac{\sin(\beta_n d/2)}{\beta_n d/2}. \tag{5a}$$

The coefficients for the transverse field components are related to e_{zn} by

$$e_{xn} = \frac{-i\beta_n}{\gamma_n} a_n e_{zn}, \tag{5b}$$

$$h_{yn} = \frac{-i\omega\epsilon_0}{\gamma_n} a_n e_{zn}, \tag{5c}$$

where the correction factor a_n is given in this case by $a_n = \cosh(\gamma_n b)/\sinh(\gamma_n b)$.

The average power flow in the empty waveguide is the sum of all the harmonic power, as a consequence of the orthogonality of the spatial harmonics. Hence

$$P = \frac{1}{\lambda_p} \int_{z=0}^{\lambda_p} \int_{x=0}^{b} E_{xo} H_{yo}^* dx\, dz = A_0^2 \sum_n \Phi_{n,n} e_{xn} h_{yn}^*. \tag{6a}$$

The coefficients $\Phi_{n,m}$ are defined for any n, m by

$$\Phi_{n,m} = \int_{x=0}^{b} \phi_{cn}(x) \phi_{cm}(x) dx. \tag{6b}$$

These coefficients can be regarded as the harmonic filling factors for $\Phi_{n,n}$, and as the cross-overlapping terms for the various harmonics, $\Phi_{n,m}|_{n \neq m}$. In a nonempty waveguide, as in the TWFEL, the various harmonics are coupled by the interaction mechanism, and the cross terms $\Phi_{n,m}$ are used then. The solution of Eq. (6b) for the functions ϕ_{cn} in Eq. (3d) results in the expression

$$\Phi_{n,m} = \frac{b}{2\cosh(\gamma_n b)\cosh(\gamma_m b)} \left(\frac{\sinh(\gamma_n + \gamma_m)b}{(\gamma_n + \gamma_m)b} + \frac{\sinh(\gamma_n - \gamma_m)b}{(\gamma_n - \gamma_m)b} \right). \tag{6c}$$

The wave description given above for the empty periodic

waveguide is used in the next section as a basis for the perturbation analysis of the TWFEL interaction.

B. The TWFEL fluid equations

We assume that, due to the TWFEL interaction, the TM wave in the periodic waveguide is growing slowly in the z direction. Hence the amplified fields are written as

$$E_x = A(z)E_{xo}, \tag{7a}$$

$$H_y = A(z)H_{yo}, \tag{7b}$$

$$E_z = A(z)E_{zo}, \tag{7c}$$

where $A(z)$ is a slowly varying amplitude and its initial value is $A(0) = A_0$. Hence the entire spatial harmonic spectrum of the amplified wave is preserved along z. Though the interaction occurs with a limited number of harmonics, all the other harmonics are amplified as well, in order to maintain the boundary conditions on the periodic waveguide walls.

A linear fluid model is derived for the TWFEL interaction in order to find the slowly varying wave amplitude $A(z)$. We begin with a standard set of linearized equations. The scalar wave equation, derived for the $\tilde{H}_y$ field component, is given by

$$\nabla^2\tilde{H}_y + k^2\tilde{H}_y = -\frac{\partial}{\partial z}\tilde{J}_x + \frac{\partial}{\partial x}\tilde{J}_z, \tag{8a}$$

where $\nabla = \hat{\mathbf{x}}\frac{\partial}{\partial x} + \hat{\mathbf{z}}\frac{\partial}{\partial z}$. The first-order components of the e-beam current, $\tilde{J}_x$ and $\tilde{J}_z$, are given by the linearized expressions

$$\tilde{J}_z = \rho_0\tilde{v}_{z1} + \tilde{\rho}_1 V_{z0}, \tag{8b}$$

$$\tilde{J}_x \cong \tilde{\rho}_1 V_W \cos(k_W z + \alpha_W). \tag{8c}$$

The relation between the e-beam density $\tilde{\rho}_1$ and the e-beam axial current $\tilde{J}_z$ is approximated by the one-dimensional (1D) continuity equation

$$\tilde{\rho}_1 \cong \frac{1}{i\omega}\frac{\partial}{\partial z}\tilde{J}_z, \tag{8d}$$

assuming that $\partial\tilde{J}_z/\partial z \gg \partial\tilde{J}_x/\partial x$. The electron first-order velocity $\tilde{v}_{z1}$ is found by the 1D Lorentz equation

$$-i\omega\tilde{v}_{z1} + V_{z0}\frac{\tilde{\partial}}{\partial z}v_{z1} = -\frac{e}{\gamma\gamma_z^2 m}\left[\tilde{E}_z + V_W\cos(k_W z + \alpha_W)\mu_0\tilde{H}_y\right], \tag{8e}$$

where $V_W = eB_W/\gamma m k_W$. The axial relativistic factor γ_z is defined as $\gamma_z = (1-\bar{\beta}_z^2)^{-1/2}$, where $\bar{\beta}_z c = V_{z0}$ is the average axial velocity of the electron.

Under the assumption of a slowly varying amplitude (7), we could replace Eq. (8a) by another scalar wave equation, either for the E_x or the E_z field components. These equations (derived from $\nabla^2\mathbf{E} + k^2\mathbf{E} = -i\omega\mu_0\mathbf{J} + \nabla\nabla\cdot\mathbf{J}/i\omega\epsilon_0$) are equivalent to (8a) and yield the same results. Equation (8a) is preferred in this case because its right-hand side (rhs) includes only first-order derivatives of the transverse and the axial current components (which correspond to the FEL and the TWT coupling, respectively), while the other equations include second-order derivatives.

The Laplace transform $\bar{A}(s) = \int_z A(z)\exp(-sz)dz$ is performed on the equation set (8a)–(8e). After some algebraic steps, Eqs. (8b) and (8d) yield an expression for the axial bunching current,

$$\tilde{\bar{J}}_z(s) = \frac{i\omega e\rho_0/V_{zo}^2}{(i\omega/V_{zo}-s)^2}\left(\tilde{\bar{E}}_z(s) + \frac{\mu_0 V_W}{2}[e^{i\alpha_W}\tilde{\bar{H}}_y(s+ik_W) + e^{-i\alpha_W}\tilde{\bar{H}}_y(s-ik_W)]\right). \tag{9a}$$

Equation (9a) shows some of the differences between the TWT, the FEL, and the TWFEL interactions. In the TWT interaction $V_W = 0$, and only the $\tilde{\bar{E}}_z$ field is included in the large parentheses on the rhs of Eq. (9a). In the FEL, only the force component $V_W\tilde{\bar{H}}_y(s+ik_W)$ [the second term in the large parentheses of Eq. (9a)] excites the bunching. In the TWFEL, however, all the components in Eq. (9a) may contribute simultaneously to the bunching process.

The TWFEL concept is applicable in both the Compton and the Raman regimes. In the latter case, the collective effect is included in the model by incorporating the axial space-charge field E_z^{ES} in the longitudinal field component E_z in Eq. (9a). Hence

$$\tilde{\bar{E}}_z = \tilde{\bar{E}}_z^{\mathrm{em}} + \tilde{\bar{E}}_z^{\mathrm{ES}}. \tag{9b}$$

The space-charge electrostatic field, neglecting its transverse components,[25] is approximated for a slowly varying amplitude by the 1D Poisson equation $\tilde{\bar{E}}_z^{\mathrm{ES}} \cong \tilde{\bar{J}}_z/i\omega\epsilon_0$. The em field component $E_z^{\mathrm{em}} = A(z)E_{zo}$ is given by Eq. (7c) for $A'/A \ll \beta_0$. Hence Eq. (9a) can be rearranged now in the form

$$\tilde{\bar{J}}_z(s) = -i\omega\epsilon_0\frac{\chi_z(s)}{1+\chi_z(s)}\{\tilde{\bar{E}}_z^{\mathrm{em}}(s) + \tfrac{1}{2}\mu_0 V_W[e^{i\alpha_W}\tilde{\bar{H}}_y(s+ik_W) + e^{-i\alpha_W}\tilde{\bar{H}}_y(s-ik_W)]\}, \tag{9c}$$

where the e-beam susceptibility $\chi_z(s)$ (for a cold e beam) and the space-charge parameter θ_p are given respectively by

$$\chi_z(s) = -\frac{\theta_p^2}{(i\omega/V_z - s)^2}, \tag{10a}$$

$$\theta_p = \left(\frac{e\rho_0}{\gamma\gamma_z^2\epsilon_0 m V_z^2}\right)^{1/2}. \tag{10b}$$

Equation (10a) corresponds to a cold electron beam. The effects of emittance and energy spread can be incorprated here by using the susceptibility terms given in Ref. 26.

The transverse current (8c) is derived by substituting Eq. (9c) into Eqs. (8c) and (8d) and is written in the form

$$\begin{aligned}\tilde{\tilde{J}}_x(s) &= \tfrac{1}{2}V_W[e^{i\alpha_W}\tilde{\rho}_1(s+ik_W) + e^{-i\alpha_W}\tilde{\rho}_1(s-ik_W)] \\ &= -\tfrac{1}{2}\epsilon_0 V_W\left(e^{i\alpha_W}(s+ik_W)\frac{\chi_z(s+ik_W)}{1+\chi_z(s+ik_W)}\{\tilde{\tilde{E}}_z^{\mathrm{em}}(s+ik_W) + \tfrac{1}{2}\mu_0 V_W[e^{i\alpha_W}\tilde{\tilde{H}}_y(s+2ik_W) + e^{-i\alpha_W}\tilde{\tilde{H}}_y(s)]\}\right. \\ &\quad + e^{-i\alpha_W}(s-ik_W)\frac{\chi_z(s-ik_W)}{1+\chi_z(s-ik_W)}\{\tilde{\tilde{E}}_z^{\mathrm{em}}(s-ik_W) \\ &\quad \left. + \tfrac{1}{2}\mu_0 V_W[e^{i\alpha_W}\tilde{\tilde{H}}_y(s) + e^{-i\alpha_W}\tilde{\tilde{H}}_y(s-2ik_W)]\}\right).\end{aligned} \tag{11}$$

The Laplace transform is performed on the wave equation (8a), and the current source terms (9c) and (11) are substituted into it. This results in

$$\begin{aligned}&\left(\frac{\partial^2}{\partial x^2} + s^2 + k^2\right)\tilde{\tilde{H}}_y(s) - s\tilde{H}_y(z)|_{z=0} - \frac{\partial}{\partial z}\tilde{H}_y(z)|_{z=0} \\ &= \tfrac{1}{2}\epsilon_0 V_W s\left[\bar{D}_s(s+ik_W)\left(e^{i\alpha_W}\tilde{\tilde{E}}_z^{\mathrm{em}}(s+ik_W) + \frac{\mu_0 V_W}{2}[e^{2i\alpha_W}\tilde{\tilde{H}}_y(s+2ik_W) + \tilde{\tilde{H}}_y(s)]\right)\right. \\ &\quad \left. + \bar{D}_s(s-ik_W)\left(e^{-i\alpha_W}\tilde{\tilde{E}}_z^{\mathrm{em}}(s-ik_W) + \frac{\mu_0 V_W}{2}[\tilde{\tilde{H}}_y(s) + e^{-2i\alpha_W}\tilde{\tilde{H}}_y(s-2ik_W)]\right)\right] \\ &\quad - i\omega\epsilon_0\bar{D}(s)\frac{\partial}{\partial x}\left(\tilde{\tilde{E}}_z^{\mathrm{em}}(s) + \frac{\mu_0 V_W}{2}[e^{i\alpha_W}\tilde{\tilde{H}}_y(s+ik_W) + e^{-i\alpha_W}\tilde{\tilde{H}}_y(s-ik_W)]\right),\end{aligned} \tag{12a}$$

where the dispersion term $\bar{D}_s(s)$ is defined for simplicity as $\bar{D}_s(s) = s\bar{D}(s)$, and

$$\bar{D}(s) = \frac{\chi_z(s)}{1+\chi_z(s)}. \tag{12b}$$

The harmonic composition of the fields (3a)–(3c) and (7a)–(7c) is written in the s plane in the form

$$\tilde{\tilde{H}}_y(s) = \sum_n h_{yn}\phi_{cn}(x)\bar{A}(s+j\beta_n), \tag{13a}$$

$$\tilde{\tilde{H}}_{yo}(s) = A_0\sum_n h_{yn}\phi_{cn}(x)\delta(s+j\beta_n). \tag{13b}$$

The wave equation (12a) is rewritten in an elaborated form, including the full harmonic dependence (13a) and (13b), as follows:

$$\begin{aligned}&\sum_n (s+i\beta_n)h_{yn}\phi_{cn}(x)[(s-i\beta_n)\bar{A}(s-i\beta_n) - A_0] \\ &= \tfrac{1}{2}\epsilon_0 V_W s\left((s+ik_W)\bar{D}(s+ik_W)\textstyle\sum_n\{e_{zn}\phi_{sn}(x)e^{i\alpha_W}\bar{A}(s-i\beta_n+ik_W)\right. \\ &\qquad + \tfrac{1}{2}\mu_0 V_W h_{yn}\phi_{cn}(x)[e^{2i\alpha_W}\bar{A}(s-i\beta_n+2ik_W) + \bar{A}(s-i\beta_n)]\} \\ &\quad + (s-ik_W)\bar{D}(s-ik_W)\sum_n\{e_{zn}\phi_{sn}(x)e^{-i\alpha_W}\bar{A}(s-i\beta_n-ik_W) \\ &\qquad \left. + \tfrac{1}{2}\mu_0 V_W h_{yn}\phi_{cn}(x)[\bar{A}(s-i\beta_n) + e^{-2i\alpha_W}\bar{A}(s-i\beta_n-2ik_W)]\}\right) \\ &\quad - i\omega\epsilon_0\bar{D}(s)\sum_n\{e_{zn}\phi'_{sn}(x)\bar{A}(s-i\beta_n) + \tfrac{1}{2}\mu_0 V_W h_{yn}\phi'_{cn}(x)[e^{i\alpha_W}\bar{A}(s-i\beta_n+ik_W) + e^{-i\alpha_W}\bar{A}(s-i\beta_n-ik_W)]\}.\end{aligned} \tag{14}$$

Equation (14) is a general wave equation for the TWFEL interaction. It can be simplified to the form of Eq. (1) by including only resonance terms in its rhs. Expressions for the coupling parameter κ are derived and studied for three different cases, $\lambda_W \neq \lambda_p, \lambda_W = 2\lambda_p$, and $\lambda_W = \lambda_p$, in the following sections.

III. COUPLING COEFFICIENTS FOR VARIOUS TWFEL INTERACTIONS

The dispersion equation (14) can be simplified to the form of Eq. (1) if the ratio between β_p and k_W is known, and if the TWFEL is operating in the vicinity of a known resonance condition. In case the e-beam velocity is synchronized with the phase velocity of one harmonic [$V_z \simeq \omega/\beta_n$, or $V_z \simeq \omega/(\beta_n + k_W)$], the corresponding susceptibility term dominates the others, which are therefore neglected. A further simplification is achieved by applying the assumption that $A(z)$ is a slowly varying amplitude. Hence an averaging operation is performed as in Eq. (6a), by convolving the complex conjugate of both sides of Eq. (14) with $E_{xo} = A_0 \sum_n e_{xn}\phi_{cn}\delta(s+j\beta_n)$, integrating over x, and taking into account only the slowly varying amplitude terms [namely, $A(s)$ for $|s| \ll k$]. This averaging in the left-hand side (lhs) of (8a) is given, in a similar manner to (6a), by

$$\frac{1}{\lambda_p}\int_{z=0}^{\lambda_p}\int_{x=0}^{b}(\nabla^2 H_y + k^2 H_y)^* E_{xo}\,dx\,dz \cong 2iA_0\frac{\partial}{\partial z}A(z)\sum_n \beta_n \Phi_{n,n} e_{xn} h_{yn}^*. \quad (15a)$$

Hence we define the normalized power coefficients of the nth harmonic as

$$p_n = \Phi_{n,n} e_{xn} h_{yn}^*, \quad (15b)$$

$$p_n' = \beta_n \Phi_{n,n} e_{xn} h_{yn}^*. \quad (15c)$$

A gain-dispersion equation in the form of Eq. (1) (Ref. 21) and the corresponding coupling terms are derived in the following sections. For the sake of simplicity, this is done first for the simpler TWFEL schemes of $\lambda_W \neq \lambda_p$, and $\lambda_W = 2\lambda_p$. This derivation provides an introduction for the more complicated analysis of the TWFEL interaction in the $\lambda_W = \lambda_p$ structure, which is the main interest of this paper. In addition to the known FEL- and TWT-type coupling terms, we obtain in the latter case complex cross-coupling terms for the hybrid TWFEL interaction.

A. FEL (or TWT) interaction with one harmonic, $\lambda_W \neq \lambda_p$

In the case of $\lambda_W \neq \lambda_p$ (and in general, $n\lambda_W \neq m\lambda_p$ for any integers n, m) there is no coincidence between the various terms in Eq. (14), since the wiggler periodicity shifting in the s plane does not coincide with the spatial harmonic span (namely, $\beta_n + lk_W \neq \beta_m$, $\forall n, m$, and $l = \pm 1, 2$). Therefore only a single waveguide harmonic may fulfill the FEL synchronism condition

$$\frac{\omega}{V_z} - \beta_n - k_W \sim 0, \quad (16a)$$

as shown in Fig. 3(a). Consequently, the dominant susceptibility term is

$$\chi_z(s+i\beta_n+ik_W) \gg \chi_z(s+i\beta_m+ilk_W) \quad \forall m \neq n \text{ or } l \neq 1, \quad (16b)$$

and only the dispersion term $\bar{D}(s + i\beta_n + ik_W)$ is in resonance in Eq. (14). Therefore only the term $\bar{D}(s + ik_W)\{[\cdots + \bar{A}(s - i\beta_n)]\}$ in the rhs of Eq. (14) contributes a significant coupling to the FEL interaction. Hence Eq.

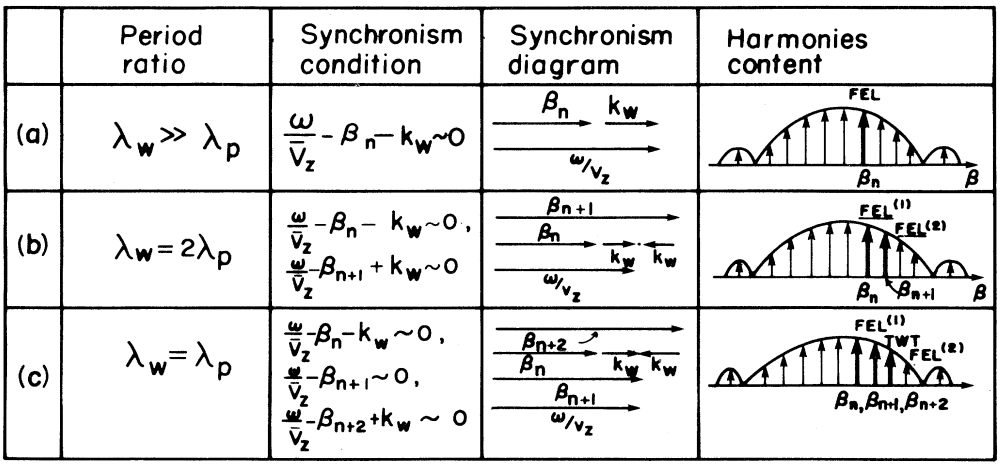

FIG. 3. Synchronism diagrams for (a) single-harmonic interaction ($\lambda_W \gg \lambda_p$), (b) two-harmonic interaction ($\lambda_W = 2\lambda_p$), and (c) three-harmonic interaction ($\lambda_W = \lambda_p$).

(14) is reduced in this case to the simpler equation

$$2i\sum_n \beta_n \Phi_{n,n} e_{x_n} h^*_{y_n}[s\bar{A}(s) - A_0]$$

$$\cong (s + i\beta_n)\frac{V_W^2}{4c^2}(s + i\beta_n + ik_W) \times \bar{D}(s + i\beta_n + ik_W)\Phi_{n,n} e_{x_n} h^*_{y_n} \bar{A}(s). \quad (17a)$$

This is further simplified to the form

$$s\bar{A}(s) - A_0 = i\kappa_n \bar{D}(s + i\beta_n + ik_W)A(s), \quad (17b)$$

where the coupling parameter for the FEL interaction with the nth harmonic is given by the expression

$$\kappa_n^{(\mathrm{FEL})} = \tfrac{1}{8}(\beta_n + k_W)\left(\frac{V_W}{c}\right)^2 C_n, \quad (18a)$$

which reveals the known FEL coupling parameter. The factor C_n is defined as

$$C_n = \frac{\beta_n \Phi_{n,n} e_{xn} h^*_{yn}}{\sum_m \beta_m \Phi_{m,m} e_{xm} h^*_{ym}} = \frac{p'_n}{\sum_m p'_m}, \quad (18b)$$

and it can be regarded as the spatial equivalent of the known JJ term for the FEL higher harmonic arising from the axial velocity modulation.[27] In terms of TWT's, C_n is related to the harmonic coupling impedance.[23]

Equation (17b) leads directly to the gain-dispersion equation

$$\bar{A}(s) = \frac{1 + \chi_z(s + i\beta_n + ik_W)}{s[1 + \chi_z(s + i\beta_n + ik_W)] - i\kappa_n \chi_z(s + i\beta_n + ik_W)} A_0. \quad (19)$$

Hence the generalized FEL gain-dispersion equation[21] is valid also for the FEL interaction with a slow harmonic in a periodic waveguide. The analysis in Ref. 22 is therefore applicable as well, using the modified coupling terms (18a) and (18b).

A TWT interaction may occur in the same scheme of $\lambda_W \neq \lambda_p$ if the e-beam velocity is tuned to satisfy the condition

$$\frac{\omega}{V_z} - \beta_n \simeq 0, \quad (20)$$

instead of the FEL tuning condition in Eq. (16a). The dominant dispersion term in this case is $\bar{D}(s + i\beta_n)$. In the averaging process of Eq. (14) only the term $s\bar{D}(s)\,[e_{z_n}\phi'_{sn}\bar{A}(s - j\beta_n)]$ contributes a significant coupling. The susceptibility term in the gain-dispersion equation (19) is replaced by $\chi_z(s + i\beta_n)$. The coupling parameter for the TWT is given then by

$$\kappa_n^{(\mathrm{TWT})} = \frac{\gamma_n^2}{2\beta_n} C_n, \quad (21)$$

in accordance with the known TWT theory.[23]

The conclusion for the case $\lambda_W \neq \lambda_p$ is that, depending on the e-beam velocity tuning, the interaction can be either an FEL interaction with a slow harmonic, or an ordinary TWT interaction. The ratio between the TWT and the FEL coupling coefficients is given by

$$\frac{\kappa_n^{(\mathrm{TWT})}}{\kappa_m^{(\mathrm{FEL})}} = \frac{4}{(V_W/c)^2}\frac{\gamma_n^2}{\beta_n(\beta_m + k_W)}\frac{C_n}{C_m}. \quad (22)$$

In all practical cases $V_W/c \ll 1$. Slow harmonics may yield $\gamma_n \simeq \beta_n$, and then the TWT interaction is stronger than the FEL interaction with the same harmonic.

B. FEL interaction with two harmonics, $\lambda_W = 2\lambda_p$

In the case of $\lambda_W = 2\lambda_p$ the spacing in the s plane between any two adjacent harmonics is $\beta_p = 2k_W$. Therefore there is a coincidence between the various $\tilde{\bar{H}}$ terms in Eq. (12a). The wiggler periodicity shifting in the s plane, by $\pm ik_W$, coincides with two adjacent spatial harmonics ($\beta_n \pm 2ik_W = \beta_{n\pm1}$). Hence two harmonics may fulfill the FEL synchronism condition in different ways, as follows:

$$\frac{\omega}{V_z} - \beta_n - k_W \simeq 0, \quad (23a)$$

$$\frac{\omega}{V_z} - \beta_{n+1} + k_W \simeq 0. \quad (23b)$$

These relations are shown as a synchronism diagram in Fig. 3(b). The harmonics of orders n and $n + 1$ both participate in the FEL interaction in this case. Consequently,

$$\chi_z(s + i\beta_n + ik_W) \gg \chi_z(s + i\beta_m + ilk_W) \quad \forall m \neq n, n+1 \text{ or } l \neq \pm 1, \quad (23c)$$

and both terms, $\bar{D}(s + i\beta_n + ik_W) = \bar{D}(s + i\beta_{n+1} - ik_W)$, are dominant. The axial field $\tilde{\bar{E}}_z^{\mathrm{em}}$ is out of resonance, and it does not fulfill here any synchronism condition. Hence no TWT interaction occurs, unless Eq. (20) is satisfied instead of Eqs. (23a) and (23b).

The averaging process is performed on Eq. (14), as in the previous case. For $\lambda_W = 2\lambda_p$, it yields

$$2\sum_n \beta_n \Phi_{n,n} e_{x_n} h^*_{y_n}[s\bar{A}(s) - A_0] = \frac{V_W^2}{4c^2}\bar{D}_s(s + i\beta_n + ik_W)\bar{A}(s) \times [\beta_n e_{x_n}(h^*_{y_n}\Phi_{n,n} + e^{2i\alpha_W} h^*_{y_{n+1}}\Phi_{n,n+1}) + \beta_{n+1} e_{x_{n+1}}(h^*_{y_{n+1}}\Phi_{n+1,n+1} + e^{-2i\alpha_W} h^*_{y_n}\Phi_{n,n+1})]. \quad (24)$$

A wave equation and a gain-dispersion equation similar to Eqs. (17b) and (19), respectivly, are accepted in this case too. However, the coupling parameter includes now the contribution of two harmonics as follows:

$$\kappa_{n,n+1}^{(\mathrm{FEL})}=\tfrac{1}{8}(\beta_n+k_W)\left(\frac{V_W}{c}\right)^2\frac{1}{\sum_n p'_n}[\beta_n\Phi_{n,n}e_{x_n}h^*_{y_n}+\hat{\beta}_{n,n+1}(\alpha_W)\Phi_{n,n+1}e_{x_n}h^*_{y_{n+1}}+\beta_{n+1}\Phi_{n+1,n+1}e_{x_{n+1}}h^*_{y_{n+1}}]. \tag{25a}$$

The first and last terms in the square brackets correspond to FEL interactions as given by Eq. (18a) for the harmonics n and $n+1$, respectively. The second term in the square brackets is a complex cross term which describes the cross coupling between the two harmonics due to the FEL interaction, where we define

$$\hat{\beta}_{n,n+1}(\alpha_W)=(\beta_n^2e^{2i\alpha_W}+\beta_{n+1}^2e^{-2i\alpha_W})/\beta_n. \tag{25b}$$

Hence the coupling coefficient (25a) can be read as

$$\kappa_{n,n+1}^{(\mathrm{FEL})}=\kappa_n^{(\mathrm{FEL})}+\kappa_{n+1}^{(\mathrm{FEL})}+\kappa_{n,n+1}^{(\mathrm{hybrid})}, \tag{25c}$$

where $\kappa_{n,n+1}^{(\mathrm{hybrid})}$ represents a hybrid term. The FEL interaction with the n harmonic, $\kappa_n^{(\mathrm{FEL})}$, is related to the resonance relation (23a), and is similar to the known FEL interaction in a uniform waveguide (or free space). The second FEL interaction, $\kappa_{n+1}^{(\mathrm{FEL})}$, occurs with the $n+1$ harmonic and is related to Eq. (23b). This resonance is possible only in a slow-wave structure because it requires $V_z > V_{\mathrm{phase}}$.

The additional hybrid term describes the synergism of the two-harmonic TWFEL interaction. The bunching caused by each harmonic is coupled also to the other harmonic by the wiggling transverse motion of the electron beam. Hence the cross-coupling term for the $n, n+1$ harmonics depends on $\Phi_{n,n+1}e_{x_n}h^*_{y_{n+1}}$ and on the complex term $\hat{\beta}_{n,n+1}(\alpha_W)$ (25b). Consequently, the synergistic TWFEL cross coupling can be tuned by modifying α_W, the relative phase between the wiggler and the periodic waveguide.

C. TWFEL interaction with three harmonics, $\lambda_W = \lambda_p$

In the case of $\lambda_W = \lambda_p$, which is the main interest of this analysis, each term in Eq. (14) may coincide with a spatial harmonic, as shown in Fig. 3(c). Hence they all participate in the TWFEL interaction. The synchronism condition can be satisfied simultaneously with three adjacent harmonics of the orders n, $n+1$, and $n+2$, as follows :

$$\frac{\omega}{V_z}-\beta_n-k_W\simeq 0, \tag{26a}$$

$$\frac{\omega}{V_z}-\beta_{n+1}\simeq 0, \tag{26b}$$

$$\frac{\omega}{V_z}-\beta_{n+2}+k_W\simeq 0. \tag{26c}$$

Equations (26a) and (26c) are equivalent to Eqs. (23a) and (23b). They describe slow and fast FEL interactions. Equation (26b), however, stands for a TWT-type interaction, and is the same as Eq. (20). Consequently, the dispersion terms for the three harmonics in resonance are equal; $\bar{D}(s+i\beta_n+ik_W)=\bar{D}(s+i\beta_{n+1})=\bar{D}(s+i\beta_{n+2}-ik_W)$, and $\chi_z(s+i\beta_{n+1})$ is considered as the dominant susceptibility term.

The wave equation for the $\lambda_W = \lambda_p$ TWFEL scheme is obtained in a process similar to the previous simpler cases. As before, it results in a wave equation and a gain-dispersion equation like Eqs. (17b) and (19), respectively. The coupling parameter κ includes additional resonance terms as follows:

$$\begin{aligned}\kappa_{n,n+1,n+2}^{(\mathrm{TWFEL})}=&\frac{1}{8\sum_m p'_m}(\beta_n+k_W)\frac{V_W^2}{c^2}[\beta_n\Phi_{n,n}e_{x_n}h^*_{y_n}+\hat{\beta}_{n,n+2}(\alpha_W)\Phi_{n,n+2}e_{x_n}h^*_{y_{n+2}}+\beta_{n+2}\Phi_{n+2,n+2}e_{x_{n+2}}h^*_{y_{n+2}}]\\&+\frac{\gamma_{n+1}^2}{2\beta_{n+1}}C_{n+1}+i\frac{V_W}{4kc\sum_m p'_m}e_{x_{n+1}}[h^*_{y_n}\beta_n^2e^{i\alpha_W}\Phi'_{n+1,n}+h^*_{y_{n+2}}\beta_{n+2}^2e^{-i\alpha_W}\Phi'_{n+1,n+2}\\&-k^2(h_{y_n}e^{-i\alpha_W}\Phi'_{n,n+1}+h_{y_{n+2}}e^{i\alpha_W}\Phi'_{n+2,n+1})].\end{aligned} \tag{27a}$$

The coefficients $\Phi'_{n,m}$ are defined, in a similar manner to Eqs. (6b) and (6c), as

$$\begin{aligned}\Phi'_{n,m}&=\int_{x=0}^{b}\phi'_{cn}(x)\phi_{cm}(x)dx\\&=\frac{\gamma_n b}{2\cosh(\gamma_n b)\cosh(\gamma_m b)}\left(\frac{\cosh(\gamma_n+\gamma_m)b-1}{(\gamma_n+\gamma_m)b}+\frac{\cosh(\gamma_n-\gamma_m)b-1}{(\gamma_n-\gamma_m)b}\right).\end{aligned} \tag{27b}$$

TABLE I. Causes of the TWFEL coupling components in Eq. (27c).

Coupling term	Bunching force	Coupled current	Interaction
$\kappa_{n+1}^{(\mathrm{TWT})}$	$F_z = -eE_z$	$J_z = \rho V_z$	TWT
$\kappa_{n,n+2}^{(\mathrm{FEL})}$	$F_z = -eV_{W_x}H_y$	$J_\perp = \rho V_\perp$	FEL
$\kappa_{n,n+1,n+2}^{(\mathrm{hybrid\ 1})}$	$F_z = -eE_z$	$J_\perp = \rho V_\perp$	TWT-FEL
$\kappa_{n,n+1,n+2}^{(\mathrm{hybrid\ 2})}$	$F_z = -eV_{W_x}H_y$	$J_z = \rho V_z$	FEL-TWT

The coupling components in Eq. (27a) incorporate both FEL and TWT features. The first three terms in the square brackets are similar to the coupling term in the previous case of $\lambda_W = 2\lambda_p$, and they can be written as $\kappa_{n,n+2}^{(\mathrm{FEL})}$ (25a). The fourth term $(\gamma_{n+1}^2/2\beta_{n+1})C_{n+1}$ is equivalent to $\kappa_{n+1}^{(\mathrm{TWT})}$ in Eq. (21), which is the TWT coupling parameter accepted in the Pierce equation.[1,23] The other coupling terms in Eq. (27a) describe the cross coupling between the FEL and TWT interactions. Hence the coupling coefficient for the $\lambda_W = \lambda_p$ TWFEL (27a) is composed of the following terms:

$$\kappa_{n,n+1,n+2}^{(\mathrm{TWFEL})} = \kappa_{n,n+2}^{(\mathrm{FEL})} + \kappa_{n+1}^{(\mathrm{TWT})} + i\kappa_{n,n+1,n+2}^{(\mathrm{hybrid\ 1})} - i\kappa_{n,n+1,n+2}^{(\mathrm{hybrid\ 2})}. \tag{27c}$$

The new hybrid 1 term is given by

$$\kappa_{n,n+1,n+2}^{(\mathrm{hybrid\ 1})} = \frac{V_W}{4kc\sum_m p'_m} e_{x_{n+1}}(h_{y_n}^* \beta_n^2 e^{i\alpha_W}\Phi'_{n+1,n} + h_{y_{n+2}}^* \beta_{n+2}^2 e^{-i\alpha_W}\Phi'_{n+1,n+2}), \tag{27d}$$

and the hybrid 2 term is given by

$$\kappa_{n,n+1,n+2}^{(\mathrm{hybrid\ 2})} = \frac{kV_W}{4c\sum_m p'_m} e_{x_{n+1}}(h_{y_n} e^{-i\alpha_W}\Phi'_{n,n+1} + h_{y_{n+2}} e^{i\alpha_W}\Phi'_{n+2,n+1}). \tag{27e}$$

The terms hybrid 1 and hybrid 2 depend on V_W/c, rather than on $(V_W/c)^2$, as the ordinary FEL coupling term. They depend also on the product of field components of adjacent harmonics $e_{x_n}h_{y_{n\pm1}}$, rather than components of the same harmonics as the uncoupled interactions. The physical causes of these complex hybrid terms (27d) and (27e) are the cross-coupling effects of the TWT and the FEL interactions.

The hybrid 1 term describes a bunched e-beam component produced by a *longitudinal* TWT mechanism (namely, by the $-eE_z$ force), but is coupled to the *transverse* em wave component as an FEL transverse current, ρV_{W_x}. The opposite occurs in the hybrid 2 coupling (27e). The bunching is produced then by an FEL ponderomotive force $(-eV_{W_x}H_y)$ and is coupled to the *longitudinal* field component by the longitudinal current ρV_z, as in the TWT. The two terms in each hybrid coupling parameter (27d) and (27e) correspond to the two harmonics $(n, n+2)$, since the TWT harmonic of order $n+1$ is coupled to two FEL harmonics of orders n and $n+2$.

The physical causes for each term in Eq. (27c), namely, the bunching force and the coupled current, are summarized in Table 1.

The TWFEL coupling (27a) is simplified in the next section for the interaction with the fundamental harmonics ($n = 0$). It is shown that the hybrid 1 coupling is comparable to the FEL and the TWT coupling.

D. Fundamental TWFEL operating mode, $\lambda_W = \lambda_p$, $n = 0$

For a TWFEL operating in the lowest-order slow harmonic, $n = 0$, the largest coupling terms in $\kappa_{0,1,2}^{(\mathrm{TWFEL})}$ (27a) are the fundamental (first) FEL term in Eq. (27a) [identical to $\kappa_n^{(\mathrm{FEL})}$ in Eq. (18a)], the TWT coupling term [the fourth term in (27a)], and the first hybrid 1 term in Eq. (27d). Hence the fundamental TWFEL operating mode is demonstrated by the simplified complex coupling coefficient

$$\kappa_{0,1}^{(\mathrm{TWFEL})} \cong \tfrac{1}{8}(\beta_0 + k_W)\left(\frac{V_W}{c}\right)^2 C_0 + \frac{\gamma_1^2}{2\beta_1}C_1 + ie^{i\alpha_W}\frac{V_W}{4kc\sum_m p'_m}\beta_0^2\Phi'_{1,0}e_{x_1}h_{y_0}^*. \tag{28}$$

A phasor diagram of the complex coupling coefficient (28) is shown in Fig. 4(a). The effect of α_W, the relative phase of the wiggler with respect to the periodic waveguide, is seen here. For $\alpha_W = 0°, 180°$ the complex term $\kappa_{0,1}^{(\mathrm{hybrid\ 1})}$ is imaginary, and is perpendicular to the real coupling terms $\kappa_0^{(\mathrm{FEL})} + \kappa_1^{(\mathrm{TWT})}$. For $\alpha_W = 270°$ this term becomes real and is positively added to the FEL and TWT coupling terms. At this point the hybrid coupling parameter attains its maximum value (hence the TWFEL hybrid coupling is in phase with the FEL and TWT uncoupled interactions). The opposite occurs when $\alpha_W = 90°$. Then the various coupling mechanisms interfere in a destructive manner.

The effect of the complex coupling parameter on the solutions of the gain-dispersion equation (1) is demonstrated here in the high-gain limit. Equation (1) is simplified in the high-gain limit to $s^3 - i\kappa\theta_p^2 = 0$.[1,21,22] Its

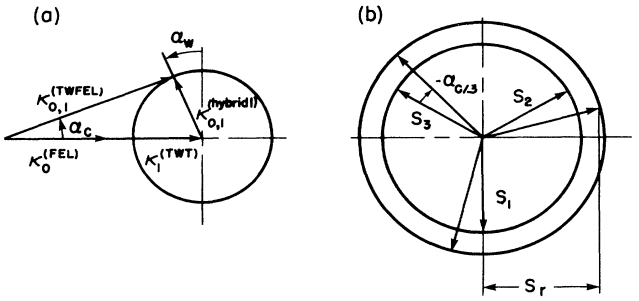

FIG. 4. The TWFEL complex coupling coefficient, and the solution of the dispersion equation (1) in the high-gain limit. (a) The phasor diagram of the complex coupling parameter in Eq. (28), $\kappa_{0,1}^{(\mathrm{TWFEL})} = \kappa_0^{(\mathrm{FEL})} + \kappa_1^{(\mathrm{TWT})} + i\kappa_{0,1,2}^{(\mathrm{hybrid\ 1})}$. The angle α_W is the relative phase of the wiggler with respect to the periodic waveguide. (b) The modification of the known zeros location of $s^3 - i\kappa\theta_p^2 = 0$ in the complex plane, due to the hybrid (complex) coupling component. The real part of the dominant solution, s_r, determines the TWFEL gain.

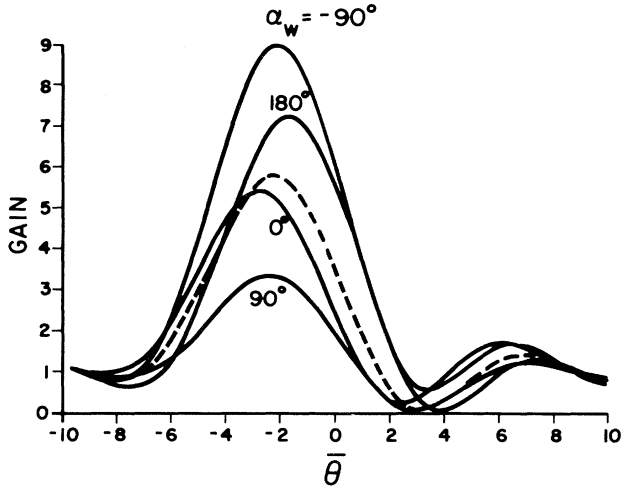

FIG. 5. Gain ($P_{\mathrm{out}}/P_{\mathrm{in}}$) vs detuning, $\bar{\theta} = (\omega/V_z - \beta_n - k_W)L_W$, for various values of α_W (the relative phase between the wiggler and the periodic waveguide). The solid curves show numerical solutions of Eq. (19) for a complex coupling, $\kappa = 10 + i4e^{i\alpha_W}$, and $\alpha_W = -90°, 0°, 90°$, and 180°. The dashed curve shows for comparison the result for a real coupling, $\kappa = 10$. (In all cases $L_W = 1$ m, and $\bar{\theta}_p = 1.0$.)

three well-known solutions in this limit are $s_1 = -iQ^{1/3}$, $s_2 = (\sqrt{3} + i)Q^{1/3}/2$, and $s_3 = (-\sqrt{3} + i)Q^{1/3}/2$. The gain parameter $Q = \kappa\theta_p^2$ is real for the ordinary TWT and FEL interactions. The TWFEL modification due the complex coupling parameter (28) is shown schematically in Fig. 4(b). The known **Y** form of the solutions $s_{1,2,3}$ in the complex plane is rotated by an angle $\alpha_c/3$, and its arm radius is modified according to the complex coupling coefficient shown in Fig. 4(a). The real part of the dominant pole s_r, shown in Fig. 4(b), determines the TWFEL amplification in the high-gain limit $G \cong |r_i \exp(s_r L_W)|^2$, where r_i is the corresponding residue of Eq. (19) and L_W is the interaction length.

The gain-dispersion equation (19) was solved numerically to demonstrate the effect of α_W, the relative phase of the wiggler with respect to the periodic waveguide. Figure 5 shows TWFEL gain curves for different values of the wiggler phase α_W. The TWFEL coupling is $\kappa = 10 + i4e^{i\alpha_W}$, for $\alpha_W = -90°$, 0°, 90°, and 180°, and $\theta_p = 1$. The difference in the various gain curves stems only from the shifting of the periodic waveguide with respect to the wiggler, and no other parameter is changed. In the case of $\alpha_W = -90°$, the TWFEL gain is about two times larger than the gain of both uncoupled TWT and FEL gain, with the same parameters. The dashed curve shows for comparison the result for a real coupling coefficient, $\kappa = 10$. Examples for practical TWFEL parameters that lead to values of coupling components of the order given above are presented in the next section.

IV. THE TWFEL AND THE MINIATURE WIGGLER CONCEPT

Conventional FEL wigglers have periods in the range of a few centimeters ($\lambda_W \sim$ 1–10 cm). These periods are much longer than the typical periods of slow-wave structures for millimeter wavelengths. Hence the use of conventional wigglers in TWFEL's is expected to be limited to the regime $\lambda_W \gg \lambda_p$, described in Sec. III A. The interaction of the electron beam with the slow wave in this case is a purely FEL type. It has the advantage of a reduced electron beam energy, but it does not include any synergistic effects.

Recently, considerable progress has been made in developing miniature wigglers with periods of a few millimeters.[28] These wigglers allow a significant reduction of the e-beam energy needed for a conventional FEL operation [as a direct result of the known relation $\lambda \cong \lambda_W/\beta(1+\beta)\gamma^2$]. The use of the miniature electromagnet wigglers introduces, however, parametric limitations on the FEL interaction; it restricts a pulse mode operation (due to thermal and mechanical constraints), and it limits the FEL electron-beam current because of the small gap between the electromagnet poles.

The miniature wiggler can be a useful component in a TWFEL device operating in the millimeter-wave regime. In a TWFEL application it may lead to a relatively short operating wavelength and a higher gain, comparing to a conventional FEL with the same low-energy and low-current electron beam. The TWFEL construction is relatively simple. The same periodic structure can be used for the wiggler and for the periodic waveguide as well (both have the same period, $\lambda_W = \lambda_p$). In the microwiggler presented in Refs. 28 and 29 the periodic structure exists already and it can be used as a base for the periodic waveguide, as well. Hence the TWFEL synergistic interaction including all the components described in Sec. III C can be realized in this device.

A miniature wiggler scheme which is applicable for TWFEL's is the folded-foil wiggler.[29] This wiggler does not contain an iron core and, therefore, the maximum magnetic field is not limited by any material saturation. Typical parameters for this design, in a pulse operation, are $\lambda_W = 4$ mm, $B_W = 4$ kG, and a wiggler parameter of $a_W = 0.15$ (peak). The TWFEL coupling coefficients computed for these wiggler parameters are presented here in a numerical example.

The slow-wave structure employed in the TWFEL example presented in this section has the dimensions $\lambda_p = 4$ mm, $d = 1$ mm, $b = 2$ mm, and $h = 6$ mm, as shown in Fig. 2. The Brillouin diagram of this periodic waveguide is shown in Fig. 6. Three frequency passbands are seen in the diagram in the ranges 0–16, 37–49, and 76–85 GHz. The slope of the dashed lines is $\pm c/2\pi$, as the wave propagation in free space. The dispersion curves meet these lines when the grooves in the periodic waveguide attain a resonance, namely, when $\lambda \cong (h - b)/2$. At these points the grooves do not impede the waveguide, and therefore $k = \beta_0$ as in free space. The diagram has a periodicity of β_p in the β dimension. Each period represents a space harmonic of the electromagnetic wave propagating in the periodic waveguide.

In the present example the TWFEL is operated in the third frequency band around $\sim$ 80 GHz (it could be operated in any other frequency band by changing the electron-beam energy). The point A in Fig. 6 shows the resonance of the FEL interaction with the first slow harmonic, and point B shows the TWT resonance. The distance between A and B is $\beta_p = k_W$, to satisfy the condition for the hybrid TWFEL interaction described in Secs. III C and III D. The dash-dotted line OB is the electron-beam curve. Its slope $\omega/[2\pi(\beta_A + k_W)] = \omega/(2\pi\beta_B)$ equals $V_z/2\pi$ as results from the TWFEL synchronism conditions (26a) and (26b).

Figure 7(a) shows the wave dispersion in the vicinity of point A (marked by a dashed box in Fig. 6). Figure 7(b) shows the electron-beam energy versus the operating frequency, as derived by the slope of the line OB. The two curves have a knee at $\sim$83 GHz. At higher frequencies the wave dispersion increases, the group velocity diminishes to zero, and the electron-beam energy drops rapidly. The electron-beam energy attains its maximum (82 keV) at $\sim$ 82 GHz, which turns out to be the optimal operating frequency in this case.

The TWFEL coupling coefficients computed for the above parameters are shown in Fig. 8. The fundamental FEL coupling $\kappa_0^{(FEL)}$ [the first term in Eq. (28)] is dominant in the frequency range below the working point A, and it drops at higher frequencies. The TWT coupling

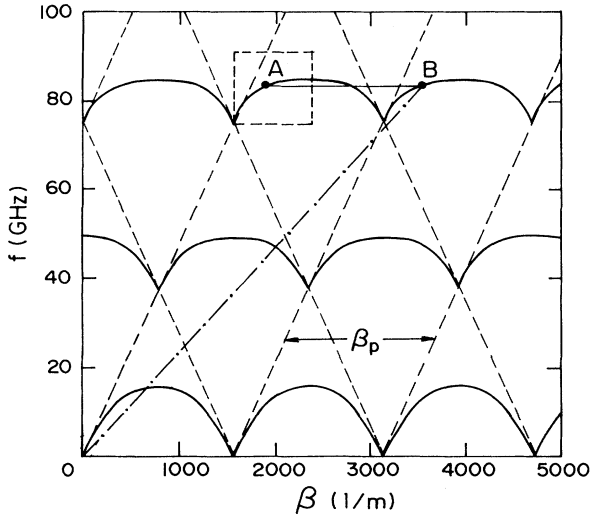

FIG. 6. A Brillouin diagram of a periodic waveguide with $\lambda_p = 4$ mm, $d = 1$ mm, $b = 2$ mm, and $h = 6$ mm. The FEL and the TWT tuning points in this example are indicated by A and B, respectively. The dash-dotted line OB is the electron-beam line corresponding to the synchronism conditions (26a) and (26b).

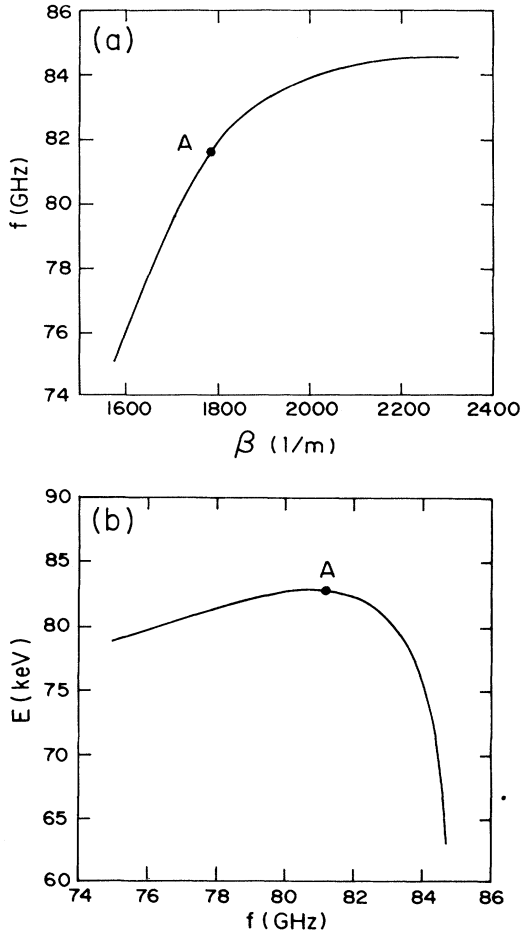

FIG. 7. Expansion of the operating point area in Fig. 6. (a) The wave dispersion in the vicinity of point A (the dashed box in Fig. 6). (b) The electron-beam energy vs the operating frequency (derived by the slope of the line OB in Fig. 6).

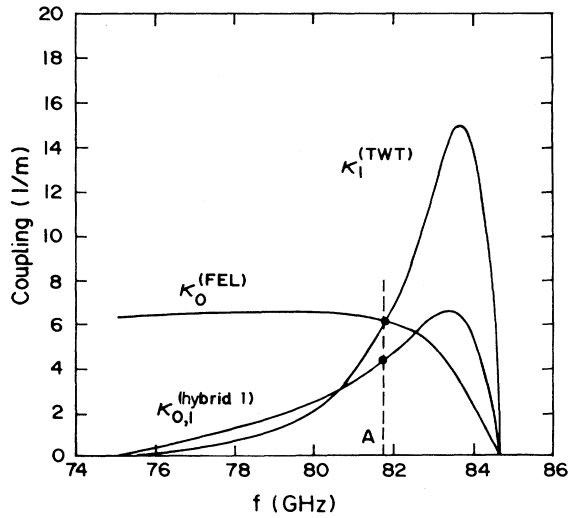

FIG. 8. The TWFEL coupling components (28): The uncoupled FEL coupling $\kappa_0^{(FEL)}$, the uncoupled TWT coupling $\kappa_1^{(TWT)}$, and the hybrid-1 coupling $|\kappa_{0,1}^{(hybrid\ 1)}|$. The wiggler parameters are $\lambda_W = 4$ mm, and $a_W = 0.15$, and the periodic waveguide dimensions are $\lambda_p = 4$ mm, $d = 1$ mm, $b = 2$ mm, and $h = 6$ mm, as in Figs. 6, 7(a) and 7(b).

$\kappa_1^{(TWT)}$ [the second term in Eq. (28)] attains its maximum and is dominant in the higher frequencies, near $\beta = 1.5\beta_p$, where the slowing effect of the periodic structure is strong and the group velocity is small. The absolute value of the TWFEL complex coupling, $\kappa_{0,1}^{(hybrid\ 1)}$ [the third term in Eq. (28)], is shown to grow moderately with the frequency and it is comparable to the FEL and TWT coupling strength in the vicinity of the optimal operating point of the TWFEL amplifier.

This example shows a typical behavior of the TWFEL coupling components. Similar results are obtained in the other frequency bands as well. The FEL fundamental coupling term is dominant near the free-space line $k = \beta_0 + n\beta_p$, whereas the TWT coupling and the hybrid-1 TWFEL coupling are negligible. The TWT coupling attains its maximum and is dominant where the dispersion is strong [near $\beta = (n+1/2)\beta_p$] and the group velocity is small. The hybrid-1 coupling coefficient resembles the TWT curve, and its strength is comparable to the FEL and TWT coupling coefficients in the vicinity of the optimal operating point.

The gain curves shown in Fig. 5 for various values of a_W correspond to TWFEL coupling values at the optimal operating point in Fig. 8 ($\kappa \cong 10 + i4e^{i\alpha_W}$). In these parameters the TWFEL gain reaches 10 dB/m at $f \sim 82$ GHz. The e-beam energy in this case is ~80 keV, and the electron beam is tenuous ($\theta_p = 1$).

This analysis has led us to conclude that the proposed TWFEL concept may be an effective mechanism for operation in the millimeter-wave regime. It can be well combined with the miniature wiggler concept and it provides enhanced interaction for low-energy and low-current electron beams. As do the other slow-wave interactions, the TWFEL requires a lower e-beam energy than *fast-wave* devices operating at the same frequencies. The TWFEL coupling is enhanced by the three-harmonic interaction, which incorporates two-harmonic FEL interactions, a TWT-type interaction, and cross-harmonic hybrid interactions. As a consequence of this enhanced coupling, the e-beam current density, or the total interaction length, needed for the TWFEL operation can be smaller than that required for the Ubitron-FEL in the same operating conditions. The TWFEL is expected therefore to be a compact amplifier for medium power millimeter radiation.

The TWFEL is being considered also as a feasible base for the FEL antenna.[30] In this device the periodic structure is made of a slot array instead of grooves. This concept is planned to be presented in another publication.

ACKNOWLEDGMENTS

The author thanks Professor George Bekefi, Professor Avi Gover, Professor Shenggang Liu, Professor Jonathan Wurtele, Professor Amitava Bhattacharjee, Ms. Toni Fisher, and Mr. Eli Aloni. This work was supported in part by the Rothschild and the Fulbright foundations.

[1] J. R. Pierce, *Travelling Wave Tube* (Van Nostrand, Princeton, 1950).
[2] R. M. Phillips, IRE Trans. **ED-7**, 231 (1960).
[3] R. M. Phillips, Nucl. Instrum. Methods A **272**, 1 (1988).
[4] H. Motz, J. Appl. Phys. **22**, 527 (1951).
[5] J. M. J. Madey, J. Appl. Phys. **42**, 1906 (1971).
[6] L. R. Elias, W. Fairbank, J. Madey, H. A. Schwettman, and T. Smith, Phys. Rev. Lett. **36**, 717 (1976).
[7] T. C. Marshall, *Free Electron Lasers* (MacMillan, New York, 1985).
[8] For recent FEL studies, see the proceedings of the FEL conferences, Nucl. Instrum. Methods A **237** (1985); **250** (1986); **258** (1987); **272** (1988).
[9] D. B. McDermott, T. C. Marshall, S. P. Schlesinger, R. K. Parker, and V. L. Granatstein, Phys. Rev. Lett. **41**, 1368 (1978).
[10] J. Fajans, G. Bekefi, Y. Z. Yin, and B. Lax, Phys. Fluids **28**, 1995 (1985).
[11] J. E. Walsh, T. C. Marshall, and S. P. Schlezinger, Phys. Fluids **20**, 709 (1977).
[12] P. Dvorkis, A. Gover, and U. Elisha, J. Opt. Soc. Am. B **1**, 723 (1984).

[13]L. Schachter and A. Ron, Appl. Phys. Lett. **53**, 828 (1988).
[14]G. Bekefi, J. S. Wurtele, and I. H. Deutsch, Phys. Rev. A **34**, 1228 (1986).
[15]J. Feinstein, A. S. Fisher, M. B. Reid, A. Ho, H. D. Dulman, and R. H. Pantell, Phys. Rev. Lett. **60**, 18 (1988).
[16]D. B. Hopkins, A. M. Sessler, and J. S. Wurtele, Nucl. Instrum. Methods **228**, 15 (1984).
[17]A. H. Ho, J. Feinstein, and R. H. Pantell, IEEE J. Quantum Electron. **QE-23**, 1545 (1987).
[18]M. A. Piestrup, IEEE J. Quantum Electron. **QE-24**, 591 (1988).
[19]E. Jerby, in *Digest of the 11th International FEL Conference, Naples, FL, 1989,* edited by L. R. Elias and I. Kimel (IEEE, New York, 1989).
[20]Shenggang Liu, in *Proceedings of the 11th International FEL Conference, Naples, FL, 1989*, edited by L. R. Elias and I. Kimel (North-Holland, Amsterdam, in press).
[21]A. Gover and P. Sprangle, IEEE J. Quantum Electron. **QE-17**, 1196 (1981).
[22]E. Jerby and A. Gover, IEEE J. Quantum Electron. **QE-21**, 1041 (1985).
[23]W. Gewartowski and G. Watson, *Microwave Tubes* (McGraw-Hill, New York, 1965).
[24]E. Aloni and E. Jerby (unpublished).
[25]E. Jerby and A. Gover, Phys. Rev. Lett. **63**, 864 (1989).
[26]E. Jerby, Nucl. Instrum. Methods A **272**, 457 (1988).
[27]W. B. Colson, IEEE J. Quantum Electron. **QE-17**, 1417 (1981).
[28]S. C. Chen, G. Bekefi, S. DiCecca, and R. Temkin, Appl. Phys. Lett. **54**, 1299 (1989), and references therein.
[29]A. Sneh and E. Jerby, Nucl. Instrum. Methods A **285**, 294 (1989).
[30]E. Jerby, Phys. Rev. A **41**, 3804 (1990).